zation.

Acknowledgment. This work was partially supported by a Grant-in-Aid for Scientific Research (No. 61540452) from the Ministry of Education, Science, and Culture of Japan.

Supplementary Material Available: Table II, listing kinetic results of the disproportion of $[Fe^{III}(CN)_4(diamine)]^-$, where diamine = (1*R*,2*S*)-*cis*-cyclohexanediamine (*cis*-chxn), (2*R*,3*S*)-butanediamine (*meso*-bn), and (2*R*,3*R*)-butanediamine (*R*-bn) (1 page). Ordering information is given on any current masthead page.

Contribution from the Department of Chemistry,
The University of Michigan, Ann Arbor, Michigan 48109

Synthesis, Structural Characterization, and Properties of the $[Mo_2O_2S_9]^{2-}$ Thio Anion and the $[Mo_4O_4S_{18}]^{2-}$, $[Mo_2O_2S_8(SCH_3)]^-$, and $[Mo_2O_2S_8Cl]^-$ Derivatives

A. I. Hadjikyriacou and D. Coucouvanis*

Received November 17, 1988

Investigation of the oxidative transformations of $[MoOS_8]^{2-}$ has led to the characterization of the Mo(VI) oxo disulfido complexes $[Mo_2O_2S_9]^{2-}$ and $[Mo_2O_2S_{10}]^{2-}$ as a solid mixture in the structure of $(Et_4N)_2[Mo_2O_2S_{9.14}]$ (I). Oxidative coupling of I affords the Mo(VI) linear tetramer $(Et_4N)_2[Mo_4O_4S_{18}]$ (III). Reaction of either I or III with $NiCl_2$ in MeCN generates the new chloro derivative $(Et_4N)[Mo_2O_2S_8Cl]$ (IV) as a result of ligand exchange. The nucleophilicity of $[Mo_2O_2S_9]^{2-}$ is demonstrated in its reaction with MeI, which gives the methanethiolato-bridged derivative $(Et_4N)[Mo_2O_2S_8(SMe)]$ (II). Both I and II crystallize in the space group $P2_1/c$ with four molecules per unit cell. The cell dimensions are a = 16.734 (2) Å, b = 10.407 (2) Å, c = 17.457 (3) Å, and β = 97.06 (1)° for I and a = 13.866 (4) Å, b = 12.927 (4) Å, c = 14.219 (4) Å, and β = 118.80 (2)° for II. Compounds III and IV crystallize in space groups $P\bar{1}$ and $P2_1/n$, respectively. The cell dimensions are a = 11.726 (3) Å, b = 12.851 (3) Å, c = 16.183 (4) Å, α = 79.21 (2)°, β = 82.68 (2)°, and γ = 79.65 (2)° for III and a = 13.309 (5) Å, b = 10.663 (3) Å, c = 16.360 (5) Å, and β = 113.74 (2)° for IV. Full-matrix refinement of 257 parameters on 3065 data for I, 208 parameters on 1803 data for II, 357 parameters on 5094 data for III, and 163 parameters on 1478 data for IV gave final R_w values of 0.064, 0.033, 0.052, and 0.037, respectively. The structures of I–IV contain Mo(VI) ions with pseudo-pentagonal-bipyramidal environments. One of the axial sites is occupied by a terminal oxo ligand. The second one is occupied by an intramolecularly weakly interacting sulfur. Two η^2-S_2^{2-} ligands and a bridging sulfur ligand define the equatorial plane of the pentagonal bipyramid. Adjacent bipyramids share the bridging ligand as common equatorial site: S^{2-} in $[Mo_2O_2S_9]^{2-}$, η^1,η^1-S_2^{2-} in $[Mo_2O_2S_{10}]^{2-}$, SMe^- in $[Mo_2O_2S_8(SMe)]^-$, η^2,η^1-S_2^{2-} in $[Mo_2O_2S_8Cl]^-$, and one η^1,η^1-S_2^{2-} and two η^2,η^1-S_2^{2-} ligands in $[Mo_4O_4S_{18}]^{2-}$. Selected bond lengths (Å): in I, Mo–Mo = 3.606 (1), Mo=O = 1.676 (6); in II, Mo–Mo = 3.570 (1), Mo–SMe = 2.525 (2), Mo=O = 1.672 (6); in III, Mo–Mo = 3.606 (1) and 3.561 (1), Mo=O = 1.676 (8), Mo–η^1,η^1-S_2 = 2.417 (3); in IV, Mo–Mo = 3.550 (1), Mo=O = 1.654, Mo–Cl = 2.388 (3). The spectroscopic properties as well as detailed synthetic procedures for I–IV are reported.

Introduction

A large body of structural and reactivity studies in molybdenum–sulfur chemistry has grown in recent years. This interest derives mainly from (a) the apparent importance of Mo–S coordination in the function of certain molybdenum-containing enzymes[1] and (b) the reactivity characteristics of "sulfided" molybdenum in the catalysis of the industrially important hydrodesulfurization (HDS) reaction.[2]

Extensive investigations in the reactivity of the tetrathiomolybdate anion, $[MoS_4]^{2-}$, have established its versatility as a bidentate ligand in the formation of heteronuclear transition-metal sulfides of the type $[M'(MoS_4)_2]^{3-}$ (M' = Co, Fe),[3] $[M'(MoS_4)_2]^{2-}$ (M' = Zn, Ni, Fe, Co, Pd, Pt),[4] and $[L_2Fe(MoS_4)]^{2-}$.[5] Further explorations in the chemistry of $[MoS_4]^{2-}$ has led to the discovery of a family of soluble binary molybdenum sulfides, $Mo_xS_y^{2-}$, that includes $[(S_4)_2MoS]^{2-}$,[6] $[(S_4)MoS(MoS_4)]^{2-}$,[7] $[(MoS_4)_2MoS]^{2-}$,[8] $[(S)_2Mo(\mu\text{-}S)]_2^{2-}$,[7] $[(S)_2Mo(\mu\text{-}S)_2MoS(\eta^2\text{-}S_2)]^{2-}$,[7] $[(\eta^2\text{-}S_2)SMo(\mu\text{-}S)]_2^{2-}$,[9] $[(\eta^2\text{-}S_2)SMo(\mu\text{-}S)_2MoS(S_4)]^{2-}$,[6,10] $[(S_4)SMo(\mu\text{-}S)]_2^{2-}$,[6,11] $[(\eta^2\text{-}S_2)_2Mo(\mu\text{-}\eta^2,\eta^2\text{-}S_2)]_2^{2-}$,[12] and $[Mo_3(\mu\text{-}S)(\mu\text{-}\eta^2,\eta^2\text{-}S_2)_3(\eta^2\text{-}S_2)_3]^{2-}$.[13]

The unique reactivity characteristics of the Mo-coordinated S_2^{2-} and S_4^{2-} ligands, toward activated alkynes or CS_2, have been explored in some detail. The reactions of dicarbalkoxyacetylenes with the S_x^{2-} ligands[14] depend on the proximal terminal ligand (O or S) attached to the Mo atom.

The reactions of the O=Mo(S_x) units in either $[(\eta^2\text{-}S_2)OMo(\mu\text{-}S)]_2^{2-}$[14b] or $[(\eta^2\text{-}S_2)OMo(\mu\text{-}S)_2MoO(S_4)]^{2-}$[14c] give rise to derivatives that contain vinyl disulfido ligands formed by the apparent insertion of the alkyne into the Mo–S_x bond. In contrast, similar reactions with the S=Mo(S_x) units in $[(S_4)_2MoS]^{2-}$ or $[(\eta^2\text{-}S_2)SMo(\mu\text{-}S)_2MoS(S_4)]^{2-}$ result in the conversion of the S_x^{2-} ligands to dithiolenes. The latter can be described formally as the result of cycloaddition to the Mo-coordinated S_x^{2-} ligands.

(1) (a) Cramer, S. P.; Stiefel, E. I. In *Molybdenum Enzymes*; Spiro, T., Ed.; Wiley: New York, 1985. (b) *Molybdenum and Molybdenum Containing Enzymes*; Coughlan, M. P., Ed.; Pergamon Press: New York, 1980.
(2) (a) Massoth, F. E. *Adv. Catal.* **1978**, *27*, 265. (b) Töpsoe, J.; Clausen, B. S. *Catal. Rev.—Sci. Eng.* **1984**, *26*, 395. (c) Weisser, O.; Landa, S. *Sulfide Catalysts: Their Properties and Applications*; Pergamon Press: London, 1973.
(3) (a) Coucouvanis, D.; Simhon, E. D.; Baenziger, N. C. *J. Am. Chem. Soc.* **1980**, *102*, 6644. (b) McDonald, J. W.; Friesen, G. D.; Newton, W. E. *Inorg. Chim. Acta.* **1980**, *46*, L79. (c) Müller, A.; Hellmann, W.; Romer, C.; Romer, M.; Bogge, H.; Jostes, R.; Schimanski, U. *Inorg. Chim. Acta* **1984**, *83*, L75. (d) Pan, W. H.; McKenna, S. T.; Chianelli, R. R.; Halbert, T. R.; Hutchings, L. L.; Stiefel, E. I. *Inorg. Chim. Acta* **1985**, *97*, L17.
(4) (a) Müller, A.; Diemann, F.; Jostes, R.; Bogge, H. *Angew. Chem., Int. Ed. Engl.* **1981**, *20*, 934. (b) Callahan, K. P.; Piliero, P. A. *Inorg. Chem.* **1980**, *19*, 2609.
(5) (a) Coucouvanis, D.; Stremple, P.; Simhon, E. D.; Swenson, D.; Baenziger, N. C.; Draganjac, M.; Chan, L. T.; Simopoulos, A.; Papaefthymiou, V.; Kostikas, A.; Petrouleas, V. *Inorg. Chem.* **1983**, *22*, 293–308. (b) Coucouvanis, D.; Baenziger, N. C.; Simhon, E. D.; Stremple, P.; Swenson, D.; Kostikas, A.; Simopoulos, A.; Petrouleas, V.; Papaefthymiou, V. *J. Am. Chem. Soc.* **1980**, *102*, 1730. (c) Coucouvanis, D.; Simhon, E. D.; Stremple, P.; Ryan, M.; Swenson, D.; Baenziger, N. C.; Simopoulos, A.; Papaefthymiou, V.; Kostikas, A.; Petrouleas, V. *Inorg. Chem.* **1984**, *23*, 741–749. (d) Coucouvanis, D. *Acc. Chem. Res.* **1981**, *14*, 201.
(6) (a) Draganjac, M.; Simhon, E.; Chan, L. T.; Kanatzidis, M.; Baenziger, N. C.; Coucouvanis, D. *Inorg. Chem.* **1982**, *21*, 3321.
(7) Hadjikyriacou, A.; Coucouvanis, D. *Inorg. Chem.* **1987**, *26*, 2400.
(8) Pan, W. H.; Leonowicz, M. E.; Stiefel, E. I. *Inorg. Chem.* **1983**, *22*, 672.
(9) (a) Miller, K. F.; Bruce, A. E.; Corbin, J. L.; Wherland, S.; Stiefel, E. I. *J. Am. Chem. Soc.* **1980**, *102*, 5102. (b) Pan, W. H.; Harmer, M. A.; Halbert, T. R.; Stiefel, E. I. *J. Am. Chem. Soc.* **1984**, *106*, 459.
(10) Clegg, W.; Christou, G.; Garner, C. D.; Sheldrick, G. M. *Inorg. Chem.* **1981**, *20*, 1562.
(11) Cohen, A.; Christou, G.; Garner, C. D.; Sheldrick, G. M. *Inorg. Chem.* **1985**, *24*, 4657.
(12) Müller, A.; Nolte, W. O.; Krebs, B. *Inorg. Chem.* **1980**, *19*, 2835.
(13) Müller, A.; Bhattacharyya, R. G.; Pfefferkorn, B. *Chem. Ber.* **1979**, *112*, 778.
(14) (a) Draganjac, M.; Coucouvanis, D. *J. Am. Chem. Soc.* **1983**, *105*, 139. (b) Halbert, T. R.; Pan, W. H.; Stiefel, E. I. *J. Am. Chem. Soc.* **1983**, *105*, 5476. (c) Coucouvanis, D.; Hadjikyriacou, A.; Draganjac, M.; Kanatzidis, M. G.; Ileperuma, O. *Polyhedron* **1986**, *5*, 349.

0020-1669/89/1328-2169$01.50/0

The reactions of the S_x^{2-} ligands in the thiodimolybdate anions and $[(S_4)_2MoS]^{2-}$ with CS_2 result in the formation of the coordinated perthiocarbonate, CS_4^{2-}, ligands.[15] These reactions, which very likely are initiated by electrophilic attack on the nucleophilic terminal sulfur atom in the Mo=S units, do not occur with the $[(S_4)_2MoO]^{2-}$ oxo thio anion.

In the hydrodesulfurization molybdenum catalysts, the nature of the active sites involved in the activation of hydrogen and the reduction of carbon–sulfur bonds has been investigated extensively.[2] Direct evidence for the participation in HDS catalysis of molybdenum-coordinated S_x^{2-} ligands is not available. However, the demonstrated reactivity of the S_x^{2-} ligands in various molybdo thio anions, and in the thoroughly investigated, tetrasulfur-bridged $[CpMo(\mu\text{-}S)_2]_2$[16] complexes, suggests the possibility of direct S_x^{2-} involvement in catalysis.

Our studies are centered on the systematic synthesis and structural characterization of Mo/S and Mo/S/O complexes and eventually an evaluation of the relative catalytic activities of these complexes in the hydrodesulfurization of thiophene. Such studies are expected to reveal the importance in HDS catalysis of "functional groups" such as Mo=O, Mo=S, $Mo(S_4)$, and $Mo(S_2)$, in various combinations and Mo oxidation states.

In this paper we report in detail the synthesis and characterization of the previously communicated[17a] $[Mo_2O_2S_{9.14}]^{2-}$ and $[Mo_4O_4S_{18}]^{2-}$ Mo(VI) oxo thio anions as well as the new derivatives $[Mo_2O_2S_8SMe]^-$ and $[Mo_2O_2S_8Cl]^-$.

Following our initial communication[17a] on the $[Mo_2O_2S_9]^{2-}$ anion, the synthesis and structural characterization of $(Me_4N)_2[Mo_2O_2S_9]$ also was reported.[17b] This compound was obtained directly from $(NH_4)_6[Mo_7O_{24}]$, $NH_2OH\cdot HCl$, and K_2S in low yield. Very recently the synthesis of the sulfur analogue of the $[Mo_2O_2S_9]^{2-}$ anion, $[Mo_2S_{11}]^{2-}$, has been claimed.[17c] The structure of the latter, however, was not determined crystallographically.

Experimental Section

General Procedures and Techniques. The chemicals in this research were used as purchased. *N,N*-Dimethylformamide, DMF, was stored over Davison 4A molecular sieves over a period of several days and then distilled over CaH_2 under reduced pressure at a temperature below 40 °C. Diethyl ether was distilled under a positive pressure of nitrogen following refluxing over fresh CaH_2 for ca. 16 h. The syntheses and purification of $(Et_4N)[Mo_2O_2S_8SMe]$, $(Et_4N)_2[Mo_4O_4S_{18}]$, and $(Et_4N)[Mo_2O_2S_8Cl]$ were carried out under nitrogen on a Schlenk line with use of dry solvents. During anaerobic procedures, solvents and solutions were transferred via cannulas with use of rubber septa. Elemental analyses on samples dried under vacuum for 6 h were carried out by Galbraith Analytical Laboratories, Knoxville, TN.

Physical Methods. Visible and UV electronic spectra were obtained on a Cary Model 219 spectrophotometer. Infrared spectra were recorded on a Nicolet 60 SX FT-IR spectrometer at a resolution of 4 cm^{-1} in compressed CsI disks. A Debye-Scherrer camera with nickel-filtered copper radiation was used to obtain X-ray powder diffraction patterns.

Preparation of Compounds. Ferrocenium Hexafluorophosphate. An amount of ferrocene (20.0 g, 0.11 mol) is dissolved in 40 mL of concentrated sulfuric acid. After it stands for 1 h, the blue solution is poured into 400 mL of water and the dilute solution is filtered through a fine-porosity fritted funnel. An aqueous solution of KPF_6 (20.0 g, 0.11 mol) is added to the filtrate, and the fine flue powdery precipitate is isolated by filtration and washed thoroughly with water, ethanol, and finally diethyl ether. The product is recrystallized from a DMF–diethyl ether mixture under nitrogen. The yield is 22 g (60%).

Bis(tetraethylammonium) Bis(tetrasulfido)oxomolybdate(IV), $(Et_4N)_2[MoOS_8]$. An amount of $(NH_4)_6Mo_7O_{24}\cdot 4H_2O$ (50.00 g, 0.046 mol) is placed in a four-L flask equipped with a Teflon-coated stirring bar. Deionized water (2000 mL) is added, and the oxomolybdate is dissolved within a few minutes of stirring. An ammonium polysulfide solution is prepared by dissolving 75.0 g of elemental sulfur in 335 mL of a 22% $(NH_4)_2S$ solution (Fisher Scientific, reagent, light, 1.060 mol). This solution is added to the oxomolybdate solution with stirring. The mixture is stirred for 1 min and then gravity-filtered into a four-L vessel containing a solution of 93.7 g of $(Et_4N)Cl\cdot 4H_2O$ (0.56 mol) in 400 mL of water. The yellow suspension so obtained is agitated and then allowed to stand for 2 h. The crude product is isolated by gravity filtration and washed thoroughly with four 100-mL portions of water, four 50-mL portions of ethanol, two 50-mL portions of CS_2, and finally two 100-mL portions of diethyl ether. The yellow-brown powder is washed with three 100-mL portions of CH_3CN to remove $(Et_4N)_2Mo_2O_2S_9$, which is a minor air oxidation byproduct.

The crude product is again washed with diethyl ether and dried under vacuum for 1 h (ambient temperature, ca. 0.1 Torr) to give ca. 130 g of yellow $(Et_4N)_2[MoOS_8]$. Finally the product is extracted in a minimal amount of DMF (ca. 500 mL per 10 g of crude product), filtered, and crystallized by the addition of 1.5 volumes of diethyl ether. The yield after drying is 101.5 g (57%) of yellow microcrystals. FT-IR (Mo=O and Mo—S vibrations, cm^{-1}): 932 (vs), 430 (w). UV–vis (DMF solution, ca 10^{-3} M, nm): 400 (sh), 316 (ϵ = 17 500). Observed X-ray powder pattern *d* spacings (Å, Cu K$\bar{\alpha}$): 8.2 (vs), 6.7 (s), 4.7 (s), 4.25 (vs). This material has the same spectroscopic properties and X-ray powder pattern as that obtained via the hydrolysis of $(Et_4N)_2[MoS_9]$.[6]

Bis(tetraethylammonium) 0.86-[(μ-Sulfido)bis(oxobis(η^2-disulfido)molybdate(VI))]-0.14-[(μ-η^1,η^1-disulfido)bis(oxobis(η^2-disulfido)molybdate(VI))], $(Et_4N)_2[(Mo_2O_2S_9)_{0.86}(Mo_2O_2S_{10})_{0.14}]$ ($(Et_4N)_2[Mo_2O_2S_{9.14}]$, I). Method a. $(Et_4N)_2[MoO(S_4)_2]$ (2.5 g, 3.97 mmol) is dissolved in acetonitrile (850 mL) to give a yellow-orange solution. Ferrocenium hexafluorophosphate, $(Cp_2Fe)PF_6$ (1.31 g, 3.96 mmol), is dissolved in DMF (15 mL) by swirling. The $(Cp_2Fe)PF_6$ solution is added to the thiomolybdate solution dropwise over a 2–3-min period. By the end of the addition of the oxidizing agent, the color of the solution is dark brown-red. The reaction mixture is stirred for 5 min more. Then it is concentrated to 30–40 mL by trap-to-trap distillation (ambient temperature to −196 °C, 0.1 Torr). The suspension obtained is vacuum-filtered to remove reaction byproducts, which are sulfur and $(Et_4N)PF_6$. The red filtrate is flooded with 2-propanol (100 mL) and placed at 0 °C. Subsequent standing for 12 h affords brown-red microcrystalline I, which is isolated by filtration and washed with two 20-mL portions of diethyl ether. It is recrystallized from MeCN–2-propanol mixtures (40 mL–100 mL) at 0 °C. The yield is 0.9 g (~60%). Anal. Calcd for $(Et_4N)_2[Mo_2O_2S_{9.14}]$: Mo, 24.74; S, 37.69; N, 3.61; C, 24.74; H, 5.15. Found: Mo, 24.64; S, 37.22; N, 3.31; C, 24.37; H, 5.15. Observed X-ray powder pattern *d* spacings (Å, Cu K$\bar{\alpha}$): 8.9 (vs), 8.1 (s), 7.5 (s), 6.3 (w), 5.6 (w), 5.0–5.2 (vs), 4.0 (w), 3.8 (w), 3.6 (w), 3.35 (w), 3.2 (w). This pattern is very nearly the same as the one calculated on the basis of the single-crystal X-ray structure determination for I.

Method b. To a vigorously stirred suspension of $(Et_4N)_2[MoOS_8]$ (10.0 g, 15.92 mmol) in 200 mL of DMF is added portionwise solid iodine (2.04 g, 8.04 mmol) over a 1–2-min period. The red-brown solution is stirred for an additional 5 min. Next it is filtered and the filtrate is flooded with 2-propanol (700 mL). The solution stands at 0 °C for 16 h, the supernatant is decanted and the precipitate washed with two 50-mL portions of ethanol, two 50-mL portions of water, a 50-mL portion of ethanol, and a 50-mL portion of diethyl ether. The precipitate is extracted in a minimal amount of MeCN and recrystallized as described in method a. The yield is 2.7 g (44%).

Tetraethylammonium (μ-Methanethiolato)bis(oxobis(η^2-disulfido)molybdate(VI)), $(Et_4N)[Mo_2O_2S_8SMe]$ (II). The compound $(Et_4N)_2[Mo_2O_2S_{9.14}]$ (2.0 g, 2.59 mmol) is dissolved in MeCN (100 mL) to give a red solution. An amount of methyl iodide (0.16 mL, 2.59 mmol) is added to the stirred thiomolybdate solution dropwise via syringe. The reaction mixture is stirred for 5 min and then filtered. The product is washed with diethyl ether and dried under vacuum. The yield is 1.1 g (65%) of brown-black II. ^1H NMR (MeCN-d_3): δ 3.56 for the SMe protons. The relative integrals of the SMe protons with respect to the cation CH_3 protons are 3:12. Observed X-ray powder pattern *d* spacings (Å, Cu K$\bar{\alpha}$): 10.0 (w), 8.8 (w), 7.4 (vs), 5.7 (m), 4.5 (w). This patern, within experimental error, is identical with the one calculated on the basis of the crystal structure determination of the $(Et_4N)[Mo_2O_2S_8SMe]$ complex.

Bis(tetraethylammonium) (μ-η^1,η^1-Disulfido)bis(tris(η^2-disulfido)dioxo(μ-η^2,η^1-disulfido)dimolybdate(VI)), $(Et_4N)_2[Mo_4O_4S_{18}]$ (III). $(Et_4N)_2[Mo_2O_2S_{9.14}]$ (1.00 g, 1.3 mmol) is completely dissolved in dry CH_3CN (40 mL). A solution of $(Cp_2Fe)PF_6$ (0.43 g, 1.30 mmol) in dry

(15) Coucouvanis, D.; Draganjac, M. *J. Am. Chem. Soc.* **1982**, *104*, 6820.
(16) (a) Rakowski-Dubois, M.; Dubois, D. L.; VanDerveer, M. C.; Haltiwanger, R. C. *Inorg. Chem.* **1981**, *20*, 3064. (b) Rakowski-Dubois, M.; VanDerveer, M. C.; Dubois, D. L.; Haltiwanger, R. C.; Miller, W. K. *J. Am. Chem. Soc.* **1983**, *105*, 7456. (c) Rakowski-Dubois, M. *J. Am. Chem. Soc.* **1983**, *105*, 3710. (d) McKenna, M.; Wright, L. L.; Miller, D. J.; Tanner, L.; Haltiwanger, R. C.; Rakowski-Dubois, M. *J. Am. Chem. Soc.* **1983**, *105*, 5329. (e) Dubois, D. L.; Miller, W. K.; Rakowski-Dubois, M. *J. Am. Chem. Soc.* **1981**, *103*, 5239. (f) Casewit, C. J.; Haltiwanger, R. C.; Noordik, J.; Rakowski-Dubois, M. *Organometallics* **1985**, *4*, 119.
(17) (a) Coucouvanis, D.; Hadjikyriacou, A. *Inorg. Chem.* **1987**, *26*, 1. (b) Xintao, W.; Shaofeng, L.; Lianyong, Z.; Quangjin, W.; Jiaxi, L. *Inorg. Chim. Acta* **1987**, *133*, 43.

CH_3CN (10 mL) is added dropwise to the stirred thiomolybdate solution within a 2–3-min period. The brown powder that precipitates is isolated by vacuum filtration. It is redissolved in DMF (40 mL) to give a deep red solution. After filtration, the solution is layered with diethyl ether (150 mL). When the solution stands for 24 h, black-red crystals form and are isolated and washed with two 20-mL portions of diethyl ether. The yield is 0.60 g (50%). Anal. Calcd for $(Et_4N)_2[Mo_4O_4S_{18}]$: Mo, 28.3; S, 42.4; C, 16.80; H, 3.46. Found: Mo, 26.86; S, 42.91; C, 16.69; H, 3.43. Observed X-ray powder pattern *d* spacings (Å, Cu K$\bar{\alpha}$): 12.5 (s), 9.2 (s), 7.9 (s), 6.8 (s), 7.2 (m), 6.2 (m), 5.8 (s), 5.4 (m), 4.95 (m), 4.7 (w), 4.4 (w), 4.2 (m), 3.6 (w), 3.1 (m). This pattern, within experimental error, is identical with the one calculated on the basis of the crystal structure determination of the $(Et_4N)_2[Mo_4O_4S_{18}]$ complex.

Tetraethylammonium (μ-η^2,η^1-Disulfido)tris(η^2-disulfido)dioxochlorodimolybdate(VI), $(Et_4N)[Mo_2O_2S_8Cl]$ (IV). To a 500-mL flask containing the compounds $(Et_4N)_2[Mo_2O_2S_{9.14}]$ (3.50 g, 4.55 mmol) and $NiCl_2$ (1.18 g, 9.10 mmol) is added CH_3CN (450 mL). The red-black suspension that is obtained is stirred for 1 h and then filtered into a 1000-mL flask. The deep red filtrate is brought to dryness by trap to trap distillation to get a red solid. This solid is washed with two 50-mL portions of methanol to remove $(Et_4N)Cl$ and a 50-mL portion of diethyl ether. The crude product is recrystallized from MeCN. The yield is 2.0 g (68%) of brown-red microcrystals. Anal. Calcd for $(Et_4N)[Mo_2O_2S_8Cl]$: S, 39.70; Cl, 5.48. Found: S, 39.64; Cl, 6.20.

X-ray Diffraction Measurements.[18] Collection and Reduction of Data. (a) $(Et_4N)_2[Mo_2O_2S_{9.14}]$ (I). Crystals suitable for X-ray measurements were grown by the slow diffusion of tetrahydrofuran into a DMF solution of I obtained according to method b with $(Cp_2Fe)PF_6$ as oxidizing agent. A brown-red crystal was mounted at the end of a glass capillary in the air. A total of 6464 reflections were collected for half a sphere of the reciprocal space to $2\theta = 45°$.

(b) $(Et_4N)[Mo_2O_2S_8SMe]$ (II). Crystals suitable for X-ray measurements were obtained by the slow diffusion of diethyl ether into a MeCN solution of II. A brown-black crystal was wedged and sealed in a glass capillary under nitrogen. A total of 2364 reflections were collected for one-fourth of a sphere of the reciprocal space to $2\theta = 40°$.

(c) $(Et_4N)_2[Mo_4O_4S_{18}]$ (III). Crystals suitable for X-ray measurements were grown by the slow diffusion of 2-propanol into a DMF solution of III. A red-black crystal was mounted at the end of a glass capillary in the air. A total of 6464 reflections were collected for half a sphere of the reciprocal space to $2\theta = 45°$.

(d) $(Et_4N)[Mo_2O_2S_8Cl]$ (IV). Crystals suitable for X-ray measurements were obtained from the slow diffusion of diethyl ether into a MeCN solution of IV obtained as described in method a. A brown-red crystal was mounted at the end of a glass capillary in the air. A total of 4377 reflections were collected for a full sphere of the reciprocal space to $2\theta = 40°$.

Solution and Refinement of Structures. (a) $(Et_4N)_2[Mo_2O_2S_{9.14}]$ (I). The coordinates of the two molybdenum atoms were determined by using the direct methods routine SOLV of the SHELXTL package (1981). These positions were verified in the Patterson map (space group $P2_1/c$). The rest of the non-hydrogen atoms were located via successive difference Fourier syntheses and refined with isotropic parameters to give R = 13.3%. At this stage the difference Fourier electron density map revealed alternative positions (S3′–S4′, S7′–S8′) for the disulfido ligands S3–S4 and S7–S8. It also showed a bridging disulfido ligand (S9′–S9″) alternative to the bridging sulfide S9. The two molybdenum atoms, the two ordered disulfido ligands, the two oxo ligands, and the bridging sulfide were refined with anisotropic temperature factors. Refinement of the occupancy factors of the disordered disulfido ligands yielded 0.644 occupancy for S3–S4 and S7–S8 and complementary occupancy of 0.356 for the alternative disulfides S3′–S4′ and S7′–S8′. The occupancy factor of the bridging sulfido ligand S9 converged to 0.856 while that of the alternative disulfido ligand S9′–S9″ converged to the complementary occupancy of 0.144. There are eight tetraethylammonium cations in the unit cell. Four of them are sitting on a general position. The other four are located on centers of symmetry (0, 0, 0; 0, $^1/_2$, $^1/_2$; $^1/_2$, 0, 0; $^1/_2$, $^1/_2$, $^1/_2$) and showed crystallographically imposed, statistical disordering of the carbon atoms. The positions of the hydrogen atoms were calculated and included in the structure factor calculation, but they were not refined. Following two additional least-squares cycles refinement converged to a weighted agreement factor of 0.064.

(b) $(Et_4N)[Mo_2O_2S_9Me]$ (II). The coordinates of the two molybdenum atoms were obtained from the Patterson map interpretation in $P2_1/c$ with a Mo1–Mo2 cross-vector at 3.55 Å. All non-hydrogen atoms were located via difference Fourier electron density maps. The negatively charged dimer is sitting on a general position. There is only one tetraethylammonium cation per asymmetric unit. It is also sitting on a general position, and it is ordered. Isotropic refinement gave R = 0.052. Both ions were refined with anisotropic temperature parameters. Refinement converged to the agreement factor R_w = 0.330. The final difference Fourier electron density map was featureless.

(c) $(Et_4N)_2[Mo_4O_4S_{18}]$ (III). The coordinates of the four molybdenum atoms were determined by using the direct methods routine SOLV of the SHELXTL package (1981). The self-vectors of the heavy atoms were identified in the Patterson map (space group $P\bar{1}$). The rest of the non-hydrogen atoms were located via successive difference Fourier electron density maps. Least-squares refinement of all non-hydrogen atoms with isotropic temperature parameters yielded R = 0.098. Although the thiomolybdate and the two cations were ordered, a DMF molecule of solvation was disordered. It was included in the structure factor calculation with fixed parameters. Anisotropic refinement of the thiomolybdate anion and one of the cations converged to final R = 0.048 and R_w = 0.052.

(d) $(Et_4N)[Mo_2O_2S_8Cl]$ (IV). The coordinates of the two molybdenum atoms were determined from the Patterson map in $P2_1/n$ with a Mo1–Mo2 cross-vector at 3.55 Å. The rest of the non-hydrogen atoms were located via successive difference Fourier electron density maps. There is one dinuclear thio anion and one cation per asymmetric unit, both sitting on general positions. Least-squares refinement at this stage yielded a conventional R value of 0.074. Refinement of the thiomolybdate ion with anisotropic temperature factors gave R = 0.055. At this stage the difference Fourier electron density map revealed two residual peaks of ca. 2 e/Å: S8X appeared 2.2 Å away from Cl1, and S1X appeared 2.1 Å away from S7. Occupancy factors of 0.85 were initially assigned to the sulfurs S1 and S8 while complementary occupancies of 0.25 were assigned to the alternative sulfurs S1X and S8X. Refinement of this model converged to a conventional R value of 0.047 with occupancies of 0.87 and 0.13 for S1, S7 and S1X, S8X, respectively. The ligand sites S2Cl and Cl1S were refined as sulfur (16e) and chloride (17e), respectively, with full occupancy factors. The positions of the hydrogen atoms were calculated and included in the structure factor calculation but were not refined. Final R = 0.039; R_w = 0.037.

Crystallographic Results. A summary of crystal data, intensity collection, and structure refinement data for compounds I–IV is given in Table I. The final atomic positional and thermal parameters are tabulated in Table II for $(Et_4N)_2[Mo_2O_2S_{9.14}]$, Table III for $(Et_4N)[Mo_2O_2S_9Me]$, Table IV for $(Et_4N)_2[Mo_4O_4S_{18}]$, and Table V for $(Et_4N)[Mo_2O_2S_8Cl]$. Selected intramolecular distances and angles are given in Tables VI and VII. The atom-labeling schemes for the thio anions of I–IV are shown in Figures 3, 6, 7, and 8, respectively.

Results and Discussion

Synthesis and Reactivity. The synthesis of the oxo(disulfido)molybdate(VI) complexes is accomplished by oxidation of the monomeric $[(S_4)_2MoO]^{2-}$ complex anion. The latter was originally prepared in low yield by the hydrolysis of the $[(S_4)_2MoS]^{2-}$ anion[6] (eq 1), and its structure has been determined.[6]

$$(Et_4N)_2[(S_4)_2MoS] + H_2O \rightarrow (Et_4N)_2[(S_4)_2MoO] + H_2S \quad (1)$$

In this paper we report on a superior procedure for the synthesis of crystalline $(Et_4N)_2[(S_4)_2MoO]$ in large quantities, under aerobic conditions. In this synthetic procedure the $[(S_4)_2MoO]^{2-}$ anion is obtained in aqueous solution by the reaction of either $[MoO_4]^{2-}$ or $[Mo_7O_{24}]^{6-}$ with ammonium polysulfide solution and rapidly isolated from the reaction medium by precipitation with the Et_4N^+

(18) Intensity data for all crystals were obtained with the use of a P3/F Nicolet four-circle automated diffractometer equipped with a graphite-crystal monochromator. All data sets were measured with the θ–2θ step-scan technique, and for all data sets the condition of the crystal was monitored by measuring three standard reflections periodically (every 90 reflections). Accurate cell parameters for all crystals were obtained from the least-squares refinement on the 2θ, ϕ, χ, and ω values of 25 machine-centered reflections with 2θ values between 25 and 45°. The raw data were reduced to net intensities, estimated standard deviations were calculated on the basis of counting statistics, Lorentz–polarization corrections were applied, and equivalent reflections were averaged. The estimated standard deviation of the structure factor was taken as the larger of that derived from counting statistics and that derived from the scatter of multiple measurements. The least-squares program used minimizes $\sum w(\Delta|F|)^2$. The weighting function used throughout the refinements of the structures gives zero weight to those reflections with $F^2 < 3\sigma(F^2)$ and $w = 1/\sigma^2(F)$ to all others; $\sigma^2(F^2) = (pF^2)^2 + \sigma_1^2(F^2)$, from counting statistics where p = 0.06. The procedures, atomic scattering factors, and anomalous dispersion corrections were used as described previously.[7] The refinement calculations were carried out on the University of Michigan Amdahl 800 computer using the locally adopted SHELXTL81 crystallographic package.

Table I. Summary of Crystal Data, Intensity Collection, and Structure Refinement Data for the $(C_2H_5)_4N^+$ Salts of $[Mo_2O_2S_{9.14}]^{2-}$ (I), $[Mo_2O_2S_9Me]^-$ (II), $[Mo_2O_4S_{18}]^{2-}$ (III), and $[Mo_2O_2S_8Cl]^-$ (IV)

	I	II	III	IV
chem formula	$C_{16}H_{40}O_4N_2Mo_2S_{9.14}$	$C_9H_{23}O_2NS_9Mo$	$C_{18}H_{47}O_5N_3Mo_4S_{18}$	$C_8H_{20}O_2NMo_2S_8Cl$
M_r	772	643.7	1357	645.5
space group	$P2_1/c$	$P2_1/c$	$P\bar{1}$	$P2_1/n$
a, Å	16.734 (2)	13.866 (4)	11.726 (3)	13.309 (5)
b, Å	10.407 (2)	12.927 (4)	12.851 (3)	10.663 (3)
c, Å	17.457 (3)	14.219 (4)	16.183 (4)	16.360 (5)
α, deg	90.00	90.00	79.21	90.00
β, deg	97.06 (1)	118.80 (2)	82.68 (2)	113.74 (2)
γ, deg	90.00	90.00	79.65 (2)	90.00
Z; V, Å^3	4; 3017	4; 2233	2; 2346	4; 2125
d_{obs}, g/cm^3 [a]	1.71	1.95	1.92	2.01
d_{calc}, g/cm^3	1.72	1.95	1.92	2.00
cryst dimens, mm		0.24 × 0.28 × 0.60		0.10 × 0.10 × 0.03
μ, cm^{-1} [b]	13.99	18.7	17.85	19.9
no. of unique rflns	3913	1917	6123	1667
no. of rflns with $I > 3\sigma$	3065	1803	5094	1478
R, R_w [c]	0.062, 0.064	0.031, 0.033	0.048, 0.052	0.039, 0.037
largest residual, e/Å^3	0.99	0.53	1.42	1.3

[a] Density determined by flotation in a CBr_4/toluene mixture. [b] Mo Kα, λ = 0.709 26 Å. [c] $R = \sum(F_o - |F_c|)/\sum F_o$; $R_w = \sum(F_o - |F_c|)^2/\sum F_o^2)^{1/2}$.

Table II. Fractional Atomic Coordinates for $(Et_4N)_2[Mo_2O_2S_{9.14}]$ (I)

atom	x	y	z	U_{eq}, [a] Å^2
Mo1	0.1592 (1)	0.5360 (1)	0.1978 (1)	0.046
Mo2	0.3621 (1)	0.5412 (1)	0.1482 (1)	0.055
S1	0.2111 (2)	0.4237 (2)	0.3115 (1)	0.057
S2	0.2825 (1)	0.5707 (2)	0.2829 (1)	0.052
S3	0.0641 (3)	0.3731 (5)	0.1638 (3)	0.055
S4	0.0920 (3)	0.4858 (5)	0.0756 (3)	0.052
S5	0.2643 (1)	0.3721 (3)	0.1253 (2)	0.060
S6	0.3706 (2)	0.3230 (3)	0.1890 (2)	0.068
S7	0.4045 (3)	0.7416 (5)	0.2117 (3)	0.060
S8	0.4771 (3)	0.5880 (6)	0.2364 (3)	0.065
S9	0.2359 (2)	0.6722 (3)	0.1154 (2)	0.062
O1	0.0989 (4)	0.6481 (6)	0.2294 (4)	0.065
O2	0.4000 (5)	0.5428 (8)	0.0638 (4)	0.098
S3′	0.0716 (5)	0.3386 (8)	0.1856 (5)	0.047
S4′	0.0773 (6)	0.4406 (10)	0.0886 (6)	0.068
S7′	0.4360 (6)	0.7126 (10)	0.2085 (5)	0.076
S8′	0.4862 (5)	0.5404 (9)	0.2402 (5)	0.053
S9′	0.1767 (11)	0.6463 (18)	0.0846 (11)	0.056
S9″	0.2905 (12)	0.7102 (19)	0.1026 (11)	0.062
N1	0.2323 (4)	1.0058 (6)	0.3419 (4)	0.043
C1	0.2349 (6)	1.0774 (9)	0.2669 (6)	0.059
C2	0.2814 (7)	1.0113 (10)	0.2099 (6)	0.068
C3	0.3175 (7)	0.9800 (11)	0.3816 (7)	0.074
C4	0.3680 (7)	1.0986 (13)	0.4000 (7)	0.086
C5	0.1873 (7)	1.0881 (9)	0.3951 (6)	0.066
C6	0.1014 (7)	1.1153 (11)	0.3629 (8)	0.082
C7	0.1899 (7)	0.8768 (10)	0.3245 (6)	0.074
C8	0.1721 (7)	0.8020 (10)	0.3958 (6)	0.074
N2	0.0	0.0	0.0	0.043
C9	−0.0922 (13)	0.0179 (20)	0.0011 (13)	0.066
C10	−0.1381 (7)	−0.1122 (12)	−0.0194 (7)	0.088
C9′	0.0397 (12)	0.1288 (21)	0.0179 (12)	0.067
C11	0.0321 (12)	−0.1139 (21)	0.0462 (12)	0.066
C12	0.0351 (15)	−0.1015 (25)	0.1324 (14)	0.070
C11′	−0.0077 (12)	0.0384 (20)	0.0896 (12)	0.062
C12′	0.0197 (15)	−0.0480 (25)	0.1461 (15)	0.072
N3	0.5	1.0	0.0	0.052
C13	0.5234 (13)	1.0907 (22)	0.0741 (13)	0.069
C14	0.5313 (9)	1.2263 (15)	0.0550 (8)	0.114
C13′	0.4958 (14)	0.8691 (23)	0.0201 (14)	0.078
C15	0.5687 (15)	1.0292 (23)	−0.0550 (14)	0.082
C16	0.6546 (16)	0.9989 (27)	−0.0113 (16)	0.085
C15′	0.5714 (13)	0.9383 (20)	0.0509 (13)	0.065
C16′	0.6495 (16)	0.9274 (27)	0.0083 (16)	0.085

[a] Equivalent isotropic U defined as one-third of the trace of the orthogonalized U_{ij} tensor.

Table III. Fractional Atomic Coordinates for $(Et_4N)[Mo_2O_2S_8(SMe)]$ (II)

atom	x	y	z	U_{eq}, [a] Å^2
Mo1	0.4273 (01)	0.6081 (01)	0.7449 (01)	0.0344
Mo2	0.1656 (01)	0.7331 (01)	0.6089 (01)	0.0302
S1	0.5642 (02)	0.6481 (02)	0.9225 (02)	0.0501
S2	0.5511 (02)	0.7512 (02)	0.8082 (02)	0.0495
S3	0.2465 (02)	0.5294 (02)	0.6680 (02)	0.0406
S4	0.3490 (02)	0.5059 (02)	0.8286 (02)	0.0524
S5	0.3138 (02)	0.7717 (02)	0.7862 (02)	0.0377
S6	0.1650 (02)	0.7376 (02)	0.7753 (02)	0.0514
S7	−0.0070 (02)	0.6465 (02)	0.5387 (02)	0.0484
S8	0.0735 (02)	0.6293 (02)	0.4522 (02)	0.0435
S9	0.3239 (02)	0.7057 (02)	0.5705 (02)	0.0372
O1	0.4929 (05)	0.5252 (05)	0.7045 (05)	0.0535
O2	0.1339 (05)	0.8521 (04)	0.5583 (04)	0.0426
C1	0.3810 (08)	0.8362 (07)	0.5754 (07)	0.0545
N1	0.1850 (05)	0.3812 (05)	0.2698 (05)	0.0330
CC1	0.0583 (07)	0.3864 (07)	0.2171 (07)	0.0445
CC2	0.0122 (08)	0.4966 (07)	0.1872 (08)	0.0523
CC3	0.2277 (07)	0.4324 (07)	0.1981 (06)	0.0419
CC4	0.1730 (08)	0.3949 (08)	0.0841 (07)	0.0539
CC5	0.2337 (07)	0.4381 (08)	0.3767 (07)	0.0462
CC6	0.3590 (08)	0.4336 (08)	0.4397 (07)	0.0558
CC7	0.2158 (08)	0.2664 (06)	0.2812 (08)	0.0487
CC8	0.1778 (08)	0.2058 (07)	0.3507 (08)	0.0612

[a] Equivalent isotropic U defined as in footnote *a* of Table II.

cation. The reaction is analogous to the reaction of $[MoS_4]^{2-}$ with dibenzyl trisulfide or elemental sulfur in the synthesis of $[(S_4)_2MoS]^{2-}$. In the above reactions the reduction of the Mo(VI) in the tetrachalcogenometalates to Mo(IV) in the $[(S_4)_2MoX]^{2-}$ products is due to internal electron transfer that accompanies the formation of S–S bonds (eq 2). Intramolecular electron transfer

$$Mo^{VI}(S)_2 \rightarrow Mo^{IV}(S_2) \qquad (2)$$

(S → Mo) induced by an external oxidant has been observed and reported in several other cases such as (a) the synthesis of $[(S_2)SMo(\mu\text{-}S)]^{2-}$ from $[MoS_4]^{2-}$ and diphenyl disulfide[9,19] and the generation of $Mo(\eta^2\text{-}S_2)(Et_2dtc)_3$ from the oxidation of $[MoS_4]^{2-}$ with tetraethylthiuram disulfide, $(Et_2dtc)_2$.[19,20] In these reactions, where the products contain molybdenum(V), bound sulfido ligands reduce both the Mo(VI) ion and the external oxidant and as a result they are oxidized to bound disulfides.

The cyclic voltammogram of $(Et_4N)_2[(S_4)_2MoO]$, in DMF solution, shows an irreversible oxidation wave at a potential less positive than that required for the oxidation of ferrocene to $(Cp_2Fe)^+$. These observations suggest that (a) the oxidized anion, $[MoOS_8]^-$, is unstable and probably transforms to a new Mo/S/O complex and (b) the $(Cp_2Fe)^+$ cation should be an appropriate

(19) Pan, W. H.; Halbert, T. R.; Hutchings, L. L.; Stiefel, E. I. *J. Chem. Soc., Chem. Commun.* **1985**, 927.
(20) Harmer, M. A.; Halbert, T. R.; Pan, W. H.; Coyle, C. L.; Cohen, S. A.; Stiefel, E. I. *Polyhedron* **1985**, *5*, 340.

Table IV. Fractional Atomic Coordinates for $(Et_4N)_2[Mo_4O_4S_{18}]$ (III)

atom	x	y	z	U_{eq},[a] Å^2
Mo1	0.2916 (01)	0.0415 (01)	0.1597 (01)	0.0426
Mo2	0.1907 (01)	0.2976 (01)	0.2264 (01)	0.0376
Mo3	0.2240 (01)	0.2786 (01)	0.5650 (01)	0.0360
Mo4	0.1259 (01)	0.0500 (01)	0.6954 (01)	0.0345
S1	0.1825 (03)	0.0790 (04)	0.0398 (02)	0.0726
S2	0.3574 (04)	0.0332 (04)	0.0148 (02)	0.0762
S3	0.3572 (03)	0.1016 (02)	0.2723 (02)	0.0421
S4	0.4834 (03)	0.0593 (03)	0.1791 (02)	0.0542
S5	0.2842 (03)	0.2703 (03)	0.0907 (02)	0.0486
S6	0.3670 (03)	0.3519 (03)	0.1559 (02)	0.0523
S7	0.1008 (03)	0.1433 (03)	0.2152 (02)	0.0451
S8	0.1054 (03)	0.1740 (03)	0.3344 (02)	0.0486
S9	0.2708 (03)	0.3546 (02)	0.3378 (02)	0.0495
S10	0.1378 (03)	0.3641 (02)	0.4364 (02)	0.0456
S11	0.3137 (03)	0.1346 (02)	0.4920 (02)	0.0445
S12	0.3193 (03)	0.0968 (02)	0.6210 (02)	0.0380
S13	0.0482 (03)	0.3822 (02)	0.6147 (02)	0.0497
S14	0.1307 (03)	0.2717 (02)	0.7056 (02)	0.0450
S15	−0.0657 (03)	0.1223 (03)	0.6614 (02)	0.0475
S16	0.0612 (03)	0.1332 (02)	0.5616 (02)	0.0437
S17	0.0556 (03)	0.0481 (03)	0.8406 (02)	0.0462
S18	0.2305 (03)	0.0494 (03)	0.8125 (02)	0.0497
O1	0.2743 (09)	−0.0837 (07)	0.2019 (06)	0.0651
O2	0.0810 (07)	0.3991 (07)	0.2025 (06)	0.0556
O3	0.3333 (07)	0.3481 (06)	0.5631 (05)	0.0512
O4	0.1478 (07)	−0.0799 (06)	0.6861 (05)	0.0448
N1	0.3109 (08)	0.7018 (07)	0.5569 (06)	0.0374
C1	0.4171 (10)	0.6934 (10)	0.6075 (08)	0.0485
C2	0.4030 (12)	0.7758 (12)	0.6653 (09)	0.0629
C3	0.2014 (11)	0.6831 (11)	0.6160 (09)	0.0564
C4	0.2085 (14)	0.5802 (12)	0.6791 (10)	0.0747
C5	0.3474 (12)	0.6153 (09)	0.4978 (08)	0.0531
C6	0.2558 (15)	0.6121 (12)	0.4428 (11)	0.0830
C7	0.2821 (12)	0.8141 (09)	0.5025 (09)	0.0546
C8	0.3803 (16)	0.8447 (11)	0.4364 (10)	0.0806
N2	0.8030 (09)	0.3133 (07)	−0.0331 (06)	0.0409
C9	0.8279 (13)	0.2642 (12)	−0.1113 (09)	0.0691
C10	0.8091 (14)	0.3414 (13)	−0.1939 (10)	0.0761
C11	0.8693 (14)	0.4070 (13)	−0.0352 (10)	0.0739
C12	1.0016 (20)	0.3748 (17)	−0.0512 (14)	0.1182
C13	0.8332 (15)	0.2218 (14)	0.0385 (11)	0.0882
C14	0.8035 (17)	0.2610 (16)	0.1278 (12)	0.1012
C15	0.6722 (13)	0.3651 (12)	−0.0238 (09)	0.0672
C16	0.5911 (17)	0.2790 (16)	−0.0186 (12)	0.1020
N3	0.5766	0.6451	0.1957	0.0600
O5	0.5922	0.4819	0.1520	0.1600
C17	0.5399	0.5507	0.1946	0.1600
C18	0.5474	0.7474	0.2207	0.1600
C19	0.6771	0.6502	0.1391	0.1600

[a] Equivalent isotropic U defined as in footnote *a* of Table II.

oxidizing reagent for the chemical oxidation of $[(S_4)_2MoO]^{2-}$. Our studies indicate that the latter proceeds according to eq 3 and 4.

$$2(Et_4N)_2[(S_4)_2MoO] + 2(Cp_2Fe)PF_6 \rightarrow (Et_4N)_2[Mo_2O_2S_9] + 2(Et_4N)PF_6 + \tfrac{7}{8}S_8 + 2Cp_2Fe \quad (3)$$

$$2(Et_4N)_2[(S_4)_2MoO] + 2(Cp_2Fe)PF_6 \rightarrow (Et_4N)_2[Mo_2O_2S_{10}] + 2(Et_4N)PF_6 + \tfrac{6}{8}S_8 + 2Cp_2Fe \quad (4)$$

In these reactions the Mo(IV) in $[(S_4)_2MoO]^{2-}$ is oxidized to Mo(VI) in the $[Mo_2O_2S_9]^{2-}$ and $[Mo_2O_2S_{10}]^{2-}$ products by only 1 equiv of external oxidant. A possible reaction pathway for these reactions is shown in Figure 1. The unstable $[(S_4)_2MoO]^-$ monoanion that forms in the 1e oxidation of $[(S_4)_2MoO]^{2-}$ undergoes internal electron transfer followed by dissociation of elemental sulfur to give the reactive $[(S_2)_2OMo^{VI}S]^-$ radical anion. Two of these radical anions couple to form $[Mo_2O_2S_{10}]^{2-}$, which upon further dissociation of elemental sulfur gives $[Mo_2O_2S_9]^{2-}$. The $(Et_4N)_2[Mo_4O_4S_{18}]$ complex (III) is obtained by the oxidative coupling of the anions in $(Et_4N)_2[Mo_2O_2S_9]$ (I) (eq 5). A possible

$$2(Et_4N)_2[Mo_2O_2S_9] + 2(Cp_2Fe)PF_6 \rightarrow (Et_4N)_2[Mo_4O_4S_{18}] + 2(Et_4N)PF_6 + 2Cp_2Fe \quad (5)$$

Table V. Fractional Atomic Coordinates for $(Et_4N)[Mo_2O_2S_8Cl]$ (IV)

atom	x	y	z	U_{eq},[a] Å^2
Mo1	0.0989 (01)	0.2494 (01)	0.9341 (01)	0.0418
Mo2	0.1701 (01)	0.1532 (01)	0.7565 (01)	0.0353
S1	0.2828 (03)	0.2835 (04)	1.0372 (03)	0.0532
S2Cl	0.1918 (03)	0.1657 (04)	1.0801 (02)	0.0696
S3	−0.0262 (02)	0.1736 (03)	0.7927 (02)	0.0441
S4	−0.0209 (03)	0.0736 (03)	0.9008 (02)	0.0621
S5	0.2360 (02)	0.0667 (03)	0.9026 (02)	0.0389
S6	0.1567 (03)	−0.0545 (03)	0.8009 (02)	0.0455
S7	0.1848 (02)	0.3511 (03)	0.8376 (02)	0.0468
S8	0.0771 (03)	0.3484 (03)	0.7062 (03)	0.0527
Cl1S	0.0511 (02)	0.0818 (03)	0.6113 (02)	0.0505
O1	0.0326 (07)	0.3726 (08)	0.9506 (05)	0.0708
O2	0.2843 (05)	0.1612 (07)	0.7406 (05)	0.0479
S1X	0.2887 (20)	0.3318 (24)	0.9698 (18)	0.0502
S8X	0.0686 (23)	0.2890 (28)	0.6429 (21)	0.0648
N1	0.1575 (06)	0.2384 (08)	0.3797 (05)	0.0333
C1	0.2637 (09)	0.2581 (10)	0.4618 (07)	0.0446
C2	0.2850 (10)	0.1598 (12)	0.5334 (08)	0.0616
C3	0.1547 (10)	0.3421 (11)	0.3162 (08)	0.0559
C4	0.0547 (11)	0.3425 (13)	0.2283 (09)	0.0730
C5	0.0573 (08)	0.2430 (10)	0.4013 (07)	0.0400
C6	0.0415 (10)	0.3609 (12)	0.4447 (08)	0.0630
C7	0.1565 (09)	0.1084 (10)	0.3389 (07)	0.0439
C8	0.2563 (10)	0.0784 (11)	0.3196 (08)	0.0598

[a] Equivalent isotropic U defined as in footnote *a* of Table II.

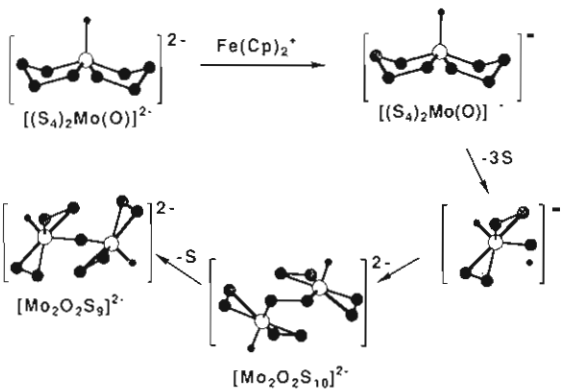

Figure 1. Possible reaction pathways for the formation of the $[Mo_2O_2S_9]^{2-}$ and $[Mo_2O_2S_{10}]^{2-}$ anions from the oxidation of the $[(S_4)_2MoO]^{2-}$ anion.

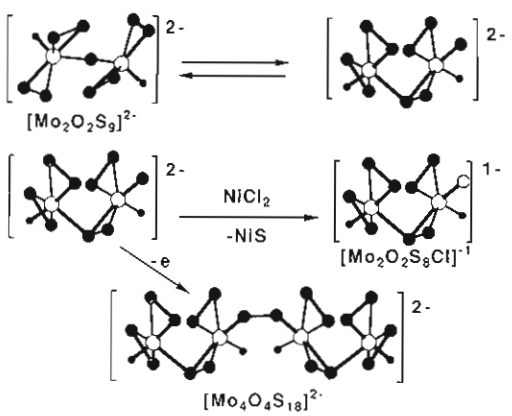

Figure 2. Proposed reaction pathways for the formation of the $[Mo_2O_2S_8Cl]^-$ and $[Mo_4O_4S_{18}]^{2-}$ anions from $[Mo_2O_2S_9]^{2-}$.

reaction pathway for this reaction is shown in Figure 2. According to this scheme reorganization of the $[Mo_2O_2S_9]^{2-}$ dianion to an intermediate with a terminal sulfido ligand and an asymmetrically bound disulfido ligand precedes the oxidative dimerization of I to the tetranuclear III. A similar intermediate may be involved in the reaction of nickel halides with I that leads to the formation of the $[Mo_2O_2S_8X]^-$ anions. The nucleophilic character of the

Table VI. Selected Bond Lengths[a] (Å) for Complexes I–IV

bond	$[Mo_2O_2S_9]^{2-}$	$[Mo_2O_2S_8SMe]^-$	$[Mo_4O_4S_{18}]^{2-}$	$[Mo_2O_2S_8Cl]^-$
Mo(1)–Mo(2)	3.606 (1)	3.570 (1)	3.606 (1)	3.550 (1)
Mo(3)–Mo(4)			3.561 (1)	
Mo–S(a)[b]	2.371 (22, 4)	2.380 (3, 2)	2.386 (4, 4)	2.377 (4, 2)
	2.377 (3, 2)	2.367 (4, 2)	2.374 (5, 4)	2.368 (9, 2)
Mo–S(b)[b]	2.409 (6, 2)	2.420 (5, 2)	2.380 (4, 4)	2.379 (3, 2)
			2.387 (7, 2)	2.392 (4)
Mo–S(c)[b]			2.457 (5, 2)	2.458 (3)
Mo–S(e)[b]	2.503 (20, 3)	2.526 (3, 2)	2.417 (3, 2)	
Mo–S(f)[b]	2.856 (3, 2)	2.843 (17, 2)	2.919 (9, 4)	2.882 (28, 2)
Mo–S(g)[b]			2.538 (8, 2)	2.535 (3)
Mo–O	1.676 (6, 2)	1.672 (6, 2)	1.676 (8, 4)	1.654 (10, 2)
Mo–Cl				2.388 (3)
S–S(a)	2.028 (8, 2)	2.037 (4, 2)	2.043 (5, 2)	2.055 (6)
S–S(b)	2.042 (4, 2)	2.046 (4, 2)	2.051 (5, 4)	2.038 (5, 2)
S–S(c)			2.055 (6, 2)	2.049 (5)
S–S(d)			2.089 (5)	
S–C		1.851 (9)		

[a] See Figures 3, 6, 7, and 8 for the atom-labeling schemes. The mean values of chemically equivalent parameters are reported. The first number in parentheses represents the larger of the standard deviations for an individual value estimated from the inverse matrix or of the standard deviation $\sigma = [\sum_{i=1}^{N}(x_i - \bar{x})^2/N(N-1)]^{1/2}$; if only two values are averaged out, the first number represents the scatter from the average. The second number in parentheses represents the independent distances averaged out. [b] The letter in parentheses corresponds to the letters in the figures in identifying the different types of S_2^{2-} bonding.

Table VII. Selected Bond Angles[a] (deg) for Complexes I–IV

angle	$[Mo_2O_2S_9]^{2-}$	$[Mo_2O_2S_8SMe]^-$	$[Mo_4O_4S_{18}]^{2-}$	$[Mo_2O_2S_8Cl]^-$
S_{eq}–Mo–O	102.1 (7, 10)	101.8 (1.0, 10)	103.3 (6, 20)	102.8 (1.1, 10)
S_{ax}–Mo–S_{eq}	78.1 (1.9, 10)	78.7 (1.6, 10)	76.8 (1.0, 20)	77.2 (1.8, 20)
S_{ax}–Mo–O	171.2 (3, 2)	168.7 (1.8, 2)	171.3 (4, 4)	171.6 (7, 2)
Mo–S_{br}–Mo	92.2 (1)	89.9 (1)	91.7 (1.0, 2)	90.6 (1)

[a] See footnote *a* in Table VI.

Table VIII. Electronic Absorptions (nm) of the Oxo(disulfido)molybdate(VI) Complexes in 10^{-3}–10^{-2} M DMF Solutions[a]

$(Et_4N)_2[(Mo_2O_2S_9)_{0.86}(Mo_2O_2S_{10})_{0.14}]$	392 (3840), 432 (4040), 522 (1950)
$(Et_4N)[Mo_2O_2S_8SMe]$	530 (2500), 436 (3000), 382 (2900), 354 (sh)
$(Et_4N)_2[Mo_4O_4S_{18}]$	338 (10450), 414 (8130), 510 (7850)
$(Et_4N)[Mo_2O_2S_8Cl]$	530 (sh), 474 (2700), 390 (sh), 350 (3000)

[a] ϵ values are given in parentheses.

bridging sulfido ligand in the $[Mo_2O_2S_9]^{2-}$ dianion is revealed in the reaction of this moiety with CH_3I (eq 6).

$$(Et_4N)_2[Mo_2O_2S_9] + CH_3I \rightarrow (Et_4N)[Mo_2O_2S_8SCH_3] + (Et_4N)I \quad (6)$$

Spectroscopic Properties. The electronic spectra of the oxo(disulfido)molybdate(VI) complexes are summarized in Table VIII. In the side-on disulfur complexes the π^* orbital of the S_2^{2-} ligand splits into two components: the in-plane π_h^* orbital and the out-of-plane π_v^* orbital. The in-plane π_h^* orbital forms a strong σ bond to the metal, leaving the π_v^* orbital at a higher energy. Two ligand to metal charge-transfer transitions are expected: $\pi_v^* \rightarrow$ d(Mo) and $\pi_h^* \rightarrow$ d(Mo). The former is observed as a low-energy absorption in the visible region. The latter is found at higher energies (due to the stabilization of the π_h^* σ-bonding orbital) in the ultraviolet region. The energies of the electronic excitations depend also on the oxidation state of the Mo and the nature of the other ligands. In several side-on disulfido complexes that contain a metal in a high oxidation state, the $\pi_v^* \rightarrow$ d(Mo) absorption is observed above 500 nm and is a diagnostic feature for the $Mo(S_2)$ functional group. In the spectrum of the complex $MoO(S_2)(Et_2NCS_2)_2$[21] the absorption at 580 nm (ϵ = 1300) has been previously assigned[22] to this LMCT. In the side-on disulfur complexes containing the $[Mo_2S_4]^{2+}$ core, a charge transfer associated with the Mo^V–S_2 fragment[6,7] is found around 560 nm. The Mo(VI) oxo disulfido complexes I–IV show several bands in the visible region. A band observed around 530 nm could be the $\pi_v^* \rightarrow$ d(Mo) LMCT, but this assignment cannot be unequivocally confirmed on the basis of the existing data.

Table IX. Infrared Spectral Data (Selected Vibrations, cm^{-1}) for the Oxo(disulfido)molybdate(VI) Complexes in CsI Disks at a Resolution of 4 cm^{-1}

$(Et_4N)_2[(Mo_2O_2S_9)_{0.86}(Mo_2O_2S_{10})_{0.14}]$	926 (vs), 528 (m), 358 (m), 352 (m), 341 (m)
$(Et_4N)[Mo_2O_2S_8SMe]$	957 (w), 939 (vs), 927 (vs), 545 (m), 535 (m), 358 (m), 347 (m)
$(Et_4N)_2[Mo_4O_4S_{18}]$	940 (vs), 930 (vs), 912 (w), 534 (m)
$(Et_4N)[Mo_2O_2S_8Cl]$	949 (s), 936 (vs), 539 (m), 378 (m), 366 (m), 297 (m)

The vibration of the terminal molybdenum–oxygen bond (Table IX) is observed in the region 910–960 cm^{-1}. The S–S vibration of the side-on disulfur ligand is found in the region 520–545 cm^{-1}. The vibration of the Mo–S single bond occurs in the far-IR region (360–290 cm^{-1}).

Structures. $(Et_4N)_2[Mo_2O_2S_{9.14}]$ (I). The crystal structure of $(Et_4N)_2[Mo_2O_2S_{9.14}]$ consists of the superposition of two different oxo thio anions, $[Mo_2O_2S_9]^{2-}$ and $[Mo_2O_2S_{10}]^{2-}$, which cocrystallize in the same lattice. Both components consist of two neutral $[MoO(S_2)_2]$ subunits bridged by either a sulfide (in $Mo_2O_2S_9^{2-}$] or a η^1,η^1-disulfide (in $Mo_2O_2S_{10}^{2-}$). They contain pseudo-seven-coordinate Mo(VI) ions with an approximate pentagonal-bipyramidal environment (Figure 3). The two η^2-S_2 ligands and the bridging sulfur ligand define the equatorial plane of the pentagonal bipyramid around each molybdenum. The two bipyramids share the bridging ligand as a common equatorial site. One of the axial sites is occupied by a terminal oxo ligand. The second one is occupied by an intramolecularly weakly interacting sulfur. The Mo–S distance associated with this interaction at ca. 2.9 Å is particularly long, and it could be attributed in part to crowding around the two bipyramids. In the $[Mo_2O_2S_9]^{2-}$ anion the two molybdenum atoms are elevated from the respective pentagonal planes by 0.47 Å.

In the structure of the nondisordered $[Mo_2O_2S_9]^{2-}$ anion[17b] the Mo–S distances for the bridging sulfide are found at 2.449 (1) and 2.469 (1) Å. The angle Mo–S_{br}–Mo is 91.59 (4)°. We believe that the long Mo–S_{br} distance observed in the structure of I at

(21) McDonald, J. W.; Newton, W. E. *Inorg. Chim. Acta* **1980**, *44*, L81.
(22) Müller, A.; Jaegermann, W.; Enemark, J. H. *Coord. Chem. Rev.* **1982**, *46*, 246.

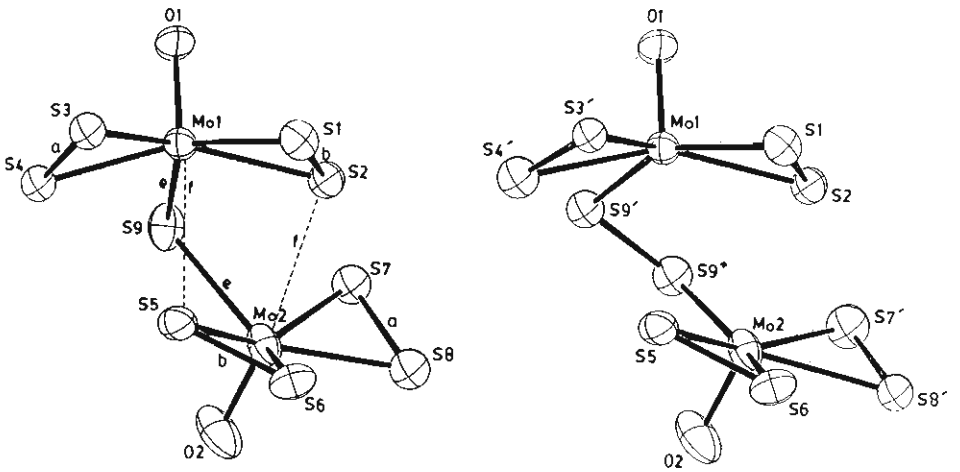

Figure 3. ORTEP drawings of the $[Mo_2O_2S_9]^{2-}$ and $[Mo_2O_2S_{10}]^{2-}$ anions in the structure of $(Et_4N)_2[Mo_2O_2S_{9.14}]$ (I). Atoms are represented by thermal ellipsoids at the 33% probability level.

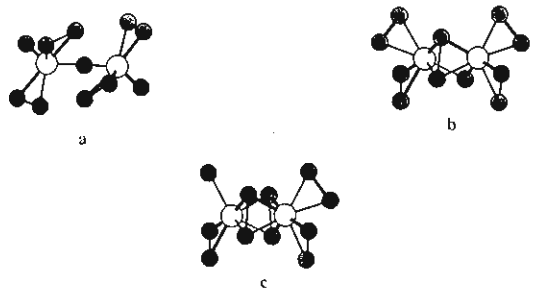

Figure 4. Possible structural isomers for the $[Mo_2S_{11}]^{2-}$ anion.

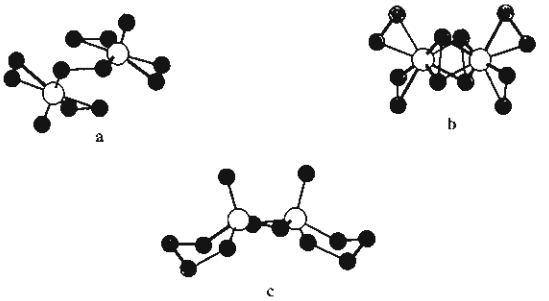

Figure 5. Structural isomers of the $[Mo_2S_{12}]^{2-}$ anion.

2.482 (6) and 2.520 (6) Å is an artifact of disorder, where ligands with different spatial demands (μ-S^{2-} and μ-η^1,η^1-S_2^{2-}) occupy the same bridging position.

The structure of $[Mo_2O_2S_9]^{2-}$ is very similar to that of the isoelectronic oxo peroxo vanadate(V) anion $[(\mu\text{-O})(VO(\eta^2\text{-}O_2)_2)_2]^{4-}$.[23] In the related pentagonal-bipyramidal oxo peroxomolybdate(VI) anion $[(\mu\text{-O})(MoO(\eta^2\text{-}O_2)_2H_2O)_2]^{2-}$,[24] the axial site (across from each terminal oxo group) is occupied by a water molecule. The complex $[Mo_2O_2S_9]^{2-}$ is also structurally analogous to the sulfido(disulfido)tungstate(VI) dimer $(Ph_4P)_2[(\mu\text{-S})(WS(\eta^2\text{-}S_2)_2)_2]$.[25]

Pentagonal-bipyramidal geometry about the seven-coordinate Mo(VI) ion is also typical in monomeric oxo(disulfido)- and oxoperoxomolybdates such as $Cs_2[MoO(\eta^2\text{-}S_2)_2$(thiooxalato-*S*,*O*)],[26] $K_2[MoO(\eta^2\text{-}O_2)_2(C_2O_4\text{-}O,O')]$,[27] and $K_2[MoO(\eta^2\text{-}O_2)_2$(glycolato-*O*,*O'*)]·$2H_2O$.[28] All the above complexes show elongation of the axial Mo–O bond across from the terminal oxo ligand. For example, in the oxoperoxo(glycolato)molybdate(VI) complex the axial position across from the terminal oxo ligand is occupied by the oxygen of the deprotonated carboxylate group of the glycolate at 2.239 (6) Å. This long axial Mo–O distance is probably due to the trans influence of the terminal oxo ligand. Crystallographic data on the seven-coordinate pentagonal-bipyramidal W(VI) monomer $WO(\eta^2\text{-}S_2)(Et_2dtc)_2$[29] show some elongation of the dithiocarbamate S—W bond (2.629 (1) Å) trans to the terminal W=O bond. Similar elongation (by less than 0.1 Å) has also been observed in the complex $WS(\eta^2\text{-}S_2)(S_2CN(i\text{-}C_4H_9)_2)_2$[19] for the dithiocarbamate S—W bond (2.588 (1) Å) trans to the terminal W=S bond. The hypothetical $[Mo_2S_{11}]^{2-}$ dimer can be envisioned in various electron redistribution forms,[7] and three of these isomers are shown in Figure 4. Only one of these

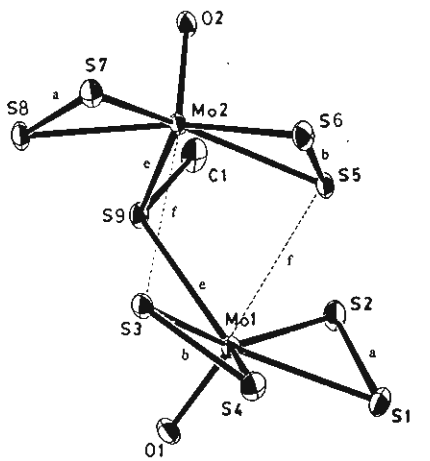

Figure 6. ORTEP drawing of the $[Mo_2O_2S_8(SMe)]^-$ monoanion of II, showing thermal ellipsoids at the 33% probability level.

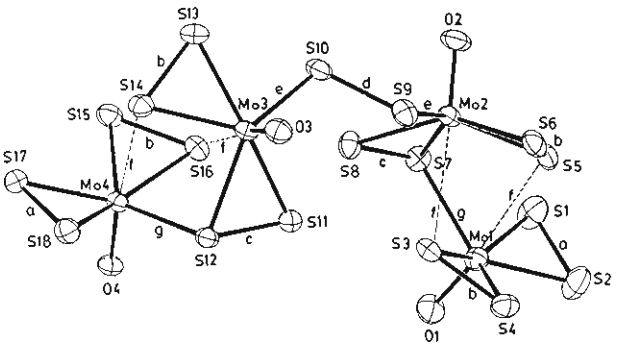

Figure 7. ORTEP drawing of the $[Mo_4O_4S_{18}]^{2-}$ dianion of III, showing thermal ellipsoids at the 33% probability level.

(23) (a) Svensson, I. B.; Stomberg, R. *Acta Chem. Scand.* **1971**, *25*, 898. (b) Stomberg, R.; Olso, S.; Svensson, I. B. *Acta Chem. Scand.* **1984**, *A38*, 653.
(24) Stomberg, R. *Acta Chem. Scand.* **1968**, *22*, 1076.
(25) Manoli, J. M.; Potvin, C.; Secheresse, F. *Inorg. Chem.* **1987**, *26*, 340.
(26) Mennemann, K.; Mattes, R. *Angew. Chem., Int. Ed. Engl.* **1977**, *16*, 260.
(27) Stomberg, R. *Acta Chem. Scand.* **1970**, *24*, 2024.
(28) Dengel, A. C.; Griffith, W. P.; Powell, R. D.; Skapski, A. C. *J. Chem. Soc., Dalton Trans.* **1987**, 991.
(29) Broomhead, J. A.; Enemark, J. H.; Hammer, B.; Ortega, R. B.; Pienkowski, W. *Aust. J. Chem.* **1987**, *40*, 381.

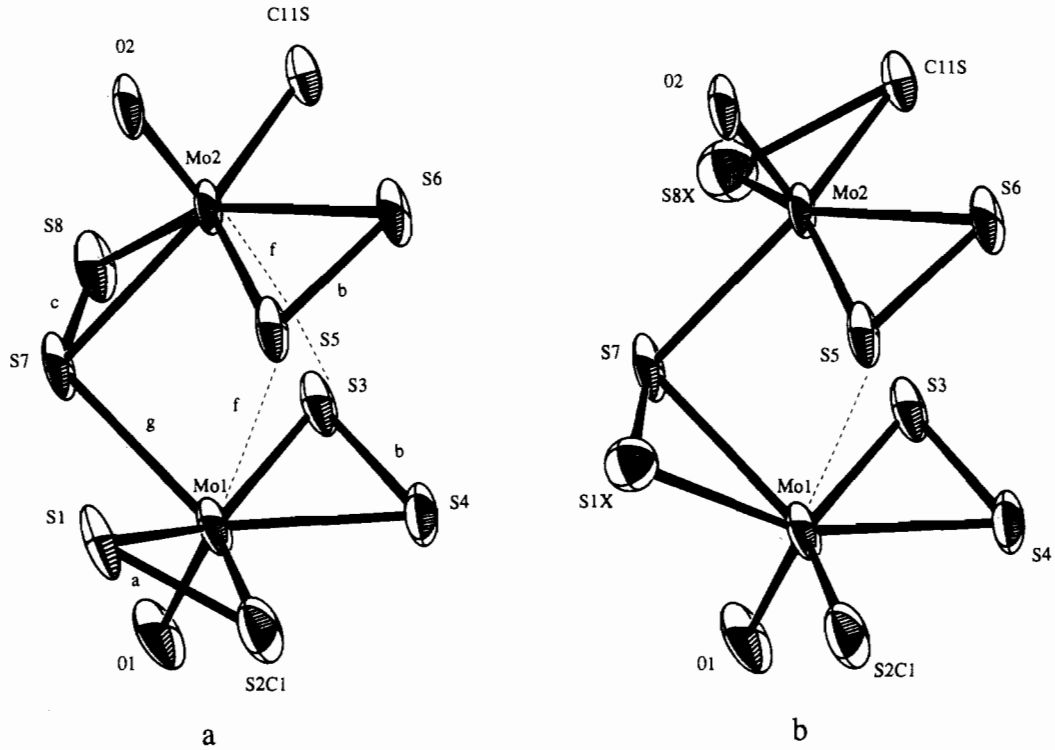

Figure 8. ORTEP drawing of the $[Mo_2O_2S_8Cl]^-$ anion of IV. The two drawings show the origin of the disorder as described in the text. S1 and S8 were refined with 0.87 occupancy and S1X and S8X with 0.13 occupancy. S2Cl and Cl1S were refined as sulfur (16e) and chlorine (17e), respectively, with full occupancy factors.

(Figure 4a) may have been synthesized.[17c] The $[Mo_2S_{12}]^{2-}$ complex anion has been characterized structurally in two electron redistribution forms, shown in parts b and c of Figure 5. The $[Mo_2S_{12}]^{2-}$ isomer with a structure similar to that of the $[O{=}Mo(S_2)_2S)_2]^{2-}$ anion (Figure 5a) has yet to be isolated.

$(Et_4N)[Mo_2O_2S_8SCH_3]$ (II). As observed in the structure of the $[Mo_2O_2S_9]^{2-}$ anion, the geometry of the Mo(VI) ions in II (Figure 6) can be described in terms of two distorted pentagonal bipyramids that share the bridging ligand as a common equatorial site. In contrast to the $[Mo_2O_2S_9]^{2-}$ anion, which contains a S^{2-} bridging ligand, the bridge in II is the CH_3S^- anion. The structural details in II are compared to those of the other thio anions I, III, and IV in Tables VI and VII. The carbon–sulfur bond length in the μ-CH_3S^- ligand, at 1.851 (9) Å, lies on the long side of the range (1.79–1.85 Å) usually observed for C–S single bonds in doubly bridging alkanethiolato complexes. In such complexes, which include $(MeCpMo(\mu\text{-}S)(\mu\text{-}SMe))_2$,[16b] $(CpMo(\mu\text{-}SMe)_2)_2$,[30] and $(MeCp_2Mo_2(\mu\text{-}S)(\mu\text{-}SMe)(\mu\text{-}\eta^2,\eta^2\text{-}S_2CH_2)]^+$,[16f] the Mo–SMe–Mo angles are very acute at 64–65°. In contrast, the corresponding angle in II is nearly 90° and probably reflects the steric crowding between the two distorted pentagonal bipyramids.

The structure of II also is related to the protonated form of the $[(\mu\text{-}O)(VO(\eta^2\text{-}O_2))_2]^{4-}$ anion $[(\mu\text{-}OH)(VO(\eta^2\text{-}O_2))_2]^{3-}$. In this complex[31] the site of protonation was identified as the bridging oxide ligand.

$(Et_4N)_2[Mo_4O_4S_{18}]$ (III). This structure (Figure 7) consists of a chain of approximate pseudo pentagonal bipyramids that share a bridging ligand as a common equatorial site. There are two different types of bridging disulfido ligands: one η^1,η^1-S_2^{2-} ligand and two η^2,η^1-S_2^{2-} ligands. The former type of ligation has been encountered in the structure of $[Me_5C_5MoS_5]_2$,[16a] where the S–S bond length for the η^1,η^1-S_2^{2-} disulfide lies at 2.040 (5) Å. The Mo–S–S–Mo moiety in III features a dihedral angle of 90° and an average Mo–S distance of 2.417 (3) Å. The S–S distance at 2.089 (5) Å is unusually long. For the majority of disulfido complexes the S–S bond length lies in the region 2.01–2.05 Å. In the complex $[(Cp(CO)_2Mn)_2(\eta^1,\eta^1\text{-}S_2)]$[32] the MnSSMn unit realizes a planar trans arrangement with a short S–S bond at 2.007 (6) Å. Planar trans arrangement has been also confirmed in the structure of $[(NH_3)_5Ru(\eta^1,\eta^1\text{-}S_2)Ru(NH_3)_5Cl_4\cdot 2H_2O$, and evidence has been presented for the formulation[33] Ru^{II}–(S_2^-)–Ru^{III}. A subsequent study[34] on the same compound describes the Ru–S–S–Ru chromophore by a qualitative orbital treatment employing the atomic orbitals of Ru(III) and the molecular orbitals of S_2^{2-} as a basis set. The structure, electrochemistry, and stoichiometry of the closely related $[R(Cp)Ru(PR_3)_2](\mu\text{-}S_2)^{2+}$[35] comlex indicate a delocalized, multiply bonded Ru–S–S–Ru planar trans core. The asymmetrical type η^2,η^1 of bridging disulfido ligand has been structurally characterized in several complexes, including $[Mo_4(NO)_4(\mu_4\text{-}S)(\mu_3\text{-}S)_2(\mu\text{-}\eta^2,\eta^1\text{-}S_2)_4(\eta^2\text{-}S_2)]^{4-}$[36] and $Cp_2Fe_2(S_2)_2(CO)$.[37]

Examination of the Mo–η^2-S_2 unit in I–IV shows two Mo–S bonds that are similar (within 3σ). In contrast, the Mo–$(\mu\text{-}\eta^2,\eta^1\text{-}S_2)$–Mo unit features three distinct types of Mo–S bonds: The longest Mo–S bond at 2.54 Å is associated with the Mo atom bound to the bridging sulfur only. The shortest Mo–S bond (2.39 Å) involves the η^1-sulfur bound to one molybdenum only. The third type of Mo–S bond lies at 2.45 Å.

$(Et_4N)[Mo_2O_2S_8Cl]$ (IV). Electron density maps showed the superposition of two dinuclear structures that are different orientations of the same molecule (Figure 8). In orientation a Mo2 is coordinated by two η^2-disulfides (S5–S6, S7–S8), a chloride (Cl1S), and an oxo ligand (O2). The disulfide S7–S8 serves as a bridge between the two molybdenum atoms in a η^2,η^1 fashion. It is bound to Mo1 via S7. Mo1 is also coordinated by two

(30) Connely, H. G.; Dahl, L. F. *J. Am. Chem. Soc.* **1970**, *92*, 7470.
(31) Campbell, N. J.; Flanagan, J.; Griffith, W. P.; Skapski, A. C. *Transition Met. Chem.* **1985**, *10*, 354.
(32) Herberhold, M.; Reiner, D.; Zimmer-Gasser, B.; Schubert, V. *Z. Naturforsch., B: Anorg. Chem., Org. Chem.* **1980**, *35B*, 1281.
(33) Elder, R. C.; Trkula, M. *Inorg. Chem.* **1977**, *16*, 1046.
(34) Kin, S.; Otterbein, E. S.; Rava, R. P.; Isied, S. S.; San Filippo, J., Jr.; Waszcyak, J. V. *J. Am. Chem. Soc.* **1983**, *105*, 336.
(35) Amarasekera, J.; Rauchfuss, T.; Wilsson, S. R. *Inorg. Chem.* **1987**, *26*, 3328.
(36) (a) Müller, A.; Eltzner, W.; Mohan, N. *Angew. Chem., Int. Ed. Engl.* **1979**, *18*, 168. (b) Müller, A.; Bhattacharyya, R. C.; Eltzner, W.; Mohan, N. *Chem. Uses Molybdenum, Proc. Int. Conf., 3rd* **1979**, 59.
(37) Gianotti, C.; Ducourant, A. M.; Chanaud, H.; Riche, C. *J. Organomet. Chem.* **1977**, *140*, 289.

η^2-disulfides (S1–S2Cl, S3–S4) and an oxo ligand (O1). This orientation is populated 87% of the time. In orientation b the disulfide S1X–S7 serves as a bridge the same way S8–S7 does in orientation a. In orientation b the ligand sites S2Cl and Cl1S are populated by a chloride and a sulfur atom, respectively. The dimer contains pseudo-seven-coordinate Mo(VI) ions. The ligands define a distorted-pentagonal-bipyramidal arrangement similar to the one observed in $[Mo_4O_4S_{18}]^{2-}$. Intramolecular bond distances and angles in IV (Tables VI and VII) are very similar to those in III. The Mo–Cl_{eq} bond length at 2.388 (3) Å is slightly shorter than the one observed in the *cis-mer* pentagonal-bipyramidal complex $Mo(O)Cl_2(Et_2NCS_2)_2$.[38] In this complex the Mo–Cl distance associated with the equatorial chloride lies at 2.417 (1) Å. In the same complex, the Mo–Cl_{ax} bond across the axial oxo ligand at 2.504 (1) Å is nearly 0.1 Å longer than the Mo–Cl_{eq} bond. This is due to the strong trans effect of the oxo group.

X-ray crystallography does not distinguish between a chloride (Cl^-) ligand and a hydrosulfido (SH^-) ligand. For this reason two formulations were considered: (a) $[Mo_2O_2S_8Cl]^-$ and (b) $[Mo_2O_2S_8SH]^-$. Formulation b would be analogous to the thiotungstate $[(\mu\text{-}\eta^2,\eta^1\text{-}S_2)W_2(S)_2(\eta^2\text{-}S_2)_3SH]^-$, $[W_2S_{11}H]^-$[39] anion. Elemental analysis for chloride indicated that formulation a is the chemically correct one. Single-crystal structure determination of the iodo analogue, $[Mo_2O_2S_8I]^-$,[40] obtained from the reaction of $(Et_4N)_2[Mo_2O_2S_{9.14}]$ with NiI_2, shows that a halide substitution for a sulfide is indeed taking place. In the structure of the $[Mo_2O_2S_8I]_2^-$ anion (R = 0.04) no disorder is encountered and, as in IV, the Mo coordination sphere geometry and the Mo—S and Mo=O bond lengths in this complex are similar to those in III. The Mo–I length is 2.766 (2) Å.

Acknowledgment. The financial support of this project by the National Science Foundation is gratefully acknowledged.

Note Added in Proof. Recently the synthesis and structural characterization of the $Ta_2S_{11}^{4-}$ and $Nb_4Se_{22}^{6-}$ anions were reported (Schreiner, S.; Aleandri, L. E.; Kang, D.; Ibers, J. A. *Inorg. Chem.* **1989**, *28*, 392). These complexes are closely related structurally to the $[Mo_2O_2S_9]^{2-}$ and $[Mo_4O_4S_{18}]^{2-}$ anions reported herein.

Supplementary Material Available: Table S1, listing thermal parameters and hydrogen atom positions for I, and Tables S2–S4, listing thermal parameters, hydrogen atom positions, and detailed bond distances and angles for II–IV (24 pages); Tables S5–S8, listing observed and calculated structure factors for I–IV (48 pages). Ordering information is given on any current masthead page.

(38) Dirand, J.; Ricard, L.; Raymond, W. *J. Chem. Soc., Dalton Trans.* **1976**, 278.
(39) Secheresse, F.; Manoli, J. M.; Potvin, C. *Inorg. Chem.* **1986**, *25*, 3967.
(40) Hadjikyriacou, A.; Coucouvanis, D. Manuscript in preparation.

Contribution from the Dow Corning Corporation, Midland, Michigan 48686

Selective and Sequential Reduction of Polyhalosilanes with Alkyltin Hydrides

John J. D'Errico† and Kenneth G. Sharp*

Received September 29, 1988

The reactions between alkyltin hydrides and a variety of polyhalo- and mixed halosilanes have been investigated. For $SiCl_4$ and $SiCl_3H$, the reductions proceed in a stepwise manner to yield the monoreduced species as the major products. The reduction of $SiBr_4$ occurs much faster to yield a mixture of $SiBr_3H$ and SiH_4, or, in the vapor phase, $SiBr_3H$ as the sole product. SiF_3X (X = Br, Cl) is converted into SiF_3H, with no further reduction of SiF_3H observed upon addition of a second equivalent of alkyltin hydride. SiF_2HX compounds (X = Br, Cl) are obtained from SiF_2X_2 and are converted into SiF_2H_2 with excess Me_3SnH. Redistribution becomes competitive with reduction in reactions between Me_3SnH and $SiFBr_3$, leading to mixtures of SiH_4, SiF_2H_2, and SiF_3H. The major products in the reaction between $SiCl_2Br_2$ and Me_3SnH are $SiCl_3H$ and SiH_4 (no $SiCl_2H_2$ was observed). Several probable intermediates were independently synthesized and allowed to react with Me_3SnH. Together with deuterium labeling experiments, these reactions shed light on the mechanisms involved in these systems. In particular, the reactions appear not to proceed via free radicals.

Introduction

Historically, the reduction of polyhalosilanes using conventional hydridic reducing agents has led to completely hydrogenated species.[1] When $LiAlH_4$ is used, it is not possible to obtain partially reduced species, even when a deficiency of the reducing agent is present. Other hydrides such as NaH and CaH_2 have been used with some success.[2,3] However, elevated temperatures (300 °C) or a catalyst such as Al_2Cl_6 is required. The latter can promote extensive redistribution reactions.

Partial substitution of hydrogen for chlorine in polychlorosilanes such as $MeSiCl_3$ can be effected via H/Cl redistribution with trialkylsilanes in the presence of catalytic quantities of Al_2Cl_6.[4] A superior catalyst—tetraalkylammonium chloride—allows H/Cl exchange between di- and triorganosilanes without skeletal participation.[5]

Organotin hydrides have long been known as effective reducing agents in organic chemistry, and their reactivity patterns have been well documented.[6] Our interest in the work described in this report lay in evaluating alkyltin hydrides as reducing agents for a variety of halosilanes.[7] A particular area of interest was the selective reduction of one halogen species to the exclusion of another in molecules such as SiF_2Br_2 and $SiCl_2Br_2$. To our knowledge, such preferential reduction of halogen has not been previously demonstrated in a polyhalosilane.

† Present address: Monsanto Chemical Co., Indian Orchard Plant, 730 Worcester St., Springfield, MA 01151.

(1) Eaborn, C. *Organosilicon Compounds*; Butterworths: London, 1960.
(2) Antipin, L.; Blekh, L.; Mironov, V. *Zh. Obshch. Khim.* **1970**, *40*, 812.
(3) Simon, G.; Lefort, M.; Birot, M.; Dunogues, J.; Duffaut, N.; Calas, R. *J. Organomet. Chem.* **1981**, *206*, 279.
(4) Whitmore, F. C.; Pietrusza, E. W.; Sommer, L. H. *J. Am. Chem. Soc.* **1947**, *69*, 2108.
(5) Weyenberg, D. R.; Bey, A. E.; Ellison, P. J. *J. Organomet. Chem.* **1965**, *3*, 489.
(6) (a) Neumann, W. P. *The Organic Chemistry of Tin*; Interscience: New York, 1970. (b) Poller, R. C. *Chemistry of Organotin Compounds*; Academic Press: New York, 1970. (c) Kupchik, E. J. In *Organotin Compounds*; Sawyer, A. K., Ed.; Marcel Dekker: New York, 1971. (d) Wardell, J. L. In *Reaction of Electrophilic Reagents with Tin Compounds Containing Organofunctional Groups*; Zuckerman, J. J., Ed.; Advances in Chemistry Series 157; American Chemical Society: Washington, DC, 1976.
(7) Although the term "reduction" should be reserved for formal changes in oxidation state, we will adhere to the usage of the term common in halosilane chemistry to describe the conversion of Si–X (X = Br, Cl) into Si–H in exchange reactions.

0020-1669/89/1328-2177$01.50/0